J. Fluid Mech. (1976), *vol.* 73, *part* 3, *pp.* 401–426
Printed in Great Britain

A rational model for Langmuir circulations

By A. D. D. CRAIK

Department of Applied Mathematics, University of St Andrews, Fife, Scotland

AND S. LEIBOVICH

Sibley School of Mechanical and Aerospace Engineering, Cornell University, Ithaca, New York 14850

(Received 19 May 1975)

A realistic theoretical model of steady Langmuir circulations is constructed. Vorticity in the wind direction is generated by the Stokes drift of the gravity-wave field acting upon spanwise vorticity deriving from the wind-driven current. We believe that the steady Langmuir circulations represent a balance between this generating mechanism and turbulent dissipation.

Nonlinear equations governing the motion are derived under fairly general conditions. Analytical and numerical solutions are sought for the case of a directional wave spectrum consisting of a single pair of gravity waves propagating at equal and opposite angles to the wind direction. Also, a statistical analysis, based on linearized equations, is developed for more general directional wave spectra. This yields an estimate of the average spacing of windrows associated with Langmuir circulations. The latter analysis is applied to a particular example with simple properties, and produces an expected windrow spacing of rather more than twice the length of the dominant gravity waves.

The relevance of our model is assessed with reference to known observational features, and the evidence supporting its applicability is promising.

1. Introduction

Langmuir circulations (abbreviated herein as LC) is the name that has been applied to sets of vortices with axes parallel to the wind direction that occur in the upper layers of lakes and the oceans. Their most obvious manifestations are windrows on the surface that are made visible by the collection of flotsam or foam, or the compression of organic films that concentrate in lines of surface convergence. The cellular motion is frequently nearly regular, with an appearance of periodicity in the cross-wind direction, and is quite vigorous. Measurements summarized by Scott *et al.* (1969) show that maximum downwelling speeds are 0·85 % of the wind velocity. Thus the strength of the downwelling motion is about one-quarter of that of the surface current induced by the wind, and one might conjecture that the vertical momentum transfer caused by LC's may play a major role in the development of the surface wind drift.

There is general agreement among those who have worked on the subject that,

as Langmuir first concluded in his pioneering paper of 1938, the circulations are driven by the wind. The driving mechanism has not, however, been satisfactorily explained to date.

Clearly the strong mixing associated with the circulations suggests that they play an important role in the energy transfer from wind to water currents and perhaps in other physical processes at the air–sea interface. On the basis of his observations that the circulations apparently penetrated to the thermocline, Langmuir originally suggested that the circulations may be the mechanism responsible for the formation of the mixed layer. One interesting and widely observed feature attributed to Langmuir circulations is the collection of oil slicks into parallel bands, a fact that has been successfully exploited in cleaning up oil spills at sea.

The importance of the circulations has been increasingly recognized, and a substantial amount of work has recently appeared relating both to observations and to attempts at theoretical explanation. We shall not review these here, but refer the interested reader to summaries appearing in Craik (1970), Faller (1971) and Scott *et al.* (1969). Our study of the literature indicates that no satisfactory theories exist and that prior to Craik's paper (1970) no ideas advanced showed promise of leading to a successful theory.

The present paper stems from that of Craik (1970) but is not subject to the criticisms levelled at that paper by Leibovich & Ulrich (1972). It is based upon the hypothesis that the circulations are a motion forced by the interaction of the vorticity in the wind-induced current and the wind-generated gravity waves. So far as the theory is concerned, the wind enters only as the source of this parallel current and of the short-crested gravity waves. The problem of the mean motion existing after the wind has been blowing for a 'long' time is specifically addressed, although it is recognized that the motion, being forced by random waves, is itself a random phenomenon.

In addition to removing the criticisms to which we have referred, the present work provides a more 'realistic' description. Recognizing that the cellular motion is not small compared with the surface wind-drift current, a set of nonlinear equations is developed by an averaging method that yields a direct representation of surface wave effects in terms of a Stokes drift. These equations are derived by consideration of vorticity and constitute an extension to viscous flows of the simple ideas of vortex-line stretching and rotation used by Leibovich & Ulrich (1972). Numerical solutions of these equations for the case of discrete wave pairs yields the correct behaviour for the downwind velocity component for sufficiently high wind speeds, and the asymmetry of the cells observed by Myer (1971) is reproduced.

Another major step towards realism involves a statistical treatment of the circulations. The analysis is restricted to a linearized form of the LC equation referred to in the previous paragraph. This equation has already been used by Craik (1970) to discuss steady Langmuir circulations. The principal outcome of the line of attack contributed here is a statistical description of the spacing of the cells generated by a spectrum of random surface waves. Thus two complementary approaches, one linearized but statistical and employing wave spectra and the other treating only motions due to a single wave pair but nonlinear, are explored.

2. Preliminary considerations

Detailed observational information concerning Langmuir circulations is not plentiful, and that which exists often raises as many equations as are answered. Nevertheless, there are some basic characteristics that seem always to be reported. We shall attempt here to summarize a minimum of features that a theory must be able to explain.

LC (1) A parallel system of vortices aligned with the wind must be predicted.

LC (2) A means must be given by which these vortices are driven by the wind.

LC (3) The resulting cells must have the possibility of an asymmetric structure with downwelling speeds larger than upwelling speeds.

LC (4) Downwelling zones must be under lines where the wind-directed surface current is greatest.

LC (5) The Langmuir circulations must have maximum downwelling speeds comparable to the mean wind-directed surface drift.

It is frequently reported that the spacing of the largest cells is fixed by the depth of the thermocline. The role of density gradients is still unclear, but the fact that LC's are observed under thermally stable conditions (Scott *et al.* 1969; Myer 1971; Langmuir 1938) suggests that density variations are a secondary feature and are not the motive force. Myer (1971), for example, clearly shows that thermal instability strengthens the LC action, while stable conditions weaken them. Langmuir's view that the thermocline is a consequence of the circulations would thus seem to gain added weight from the more extensive modern measurements.

Pre-existing sharp density gradients might nevertheless play an important role in establishing the spacing of the cells. Assaf, Gerard & Gordon (1971) reported on systems of LC's in the ocean off Bermuda. The largest scales were comparable to the depth of the mixed layer, but a series of smaller scales coexisted with them. Langmuir (1938) reported the same thing: "...between well-defined streaks there are numerous smaller and less well-defined streaks. Just as large waves have smaller waves upon them, it appears that the surfaces of the larger vortices contain smaller and shallower vortices".

In our treatment the water is taken to have constant density. For regular wave fields (such as the oblique wave pairs considered by Craik 1970) a well-defined spacing necessarily occurs. On the other hand, the cell spacing engendered by a complex wave system is related to the statistical properties of the wave field. Both situations will be considered here.

Diffusion (of momentum and vorticity) is an essential process for a steady-state solution, and is incorporated in the model. In reality, diffusion will mostly be effected by turbulence. For simplicity, we represent these effects by a constant eddy viscosity model. The 'eddy viscosity' in the ocean is probably not constant, but there seems to be no model capable of relating turbulence in the water to wind speed (as we should like to do) with a more secure basis.

Semi-empirical theories concerned with the mutual effects of waves and turbulence typically connect the eddy viscosity with a characteristic wave slope

(measured here by the parameter ϵ). (See, for example, Bowden 1950; Ichiye 1967.) We shall assume here that there is a connexion that may be expressed as

$$\nu_e = \alpha\epsilon^2, \tag{1}$$

where α is independent of ϵ.† Indeed, the existence of a steady $O(\epsilon^2)$ secondary flow (driven by undamped waves) seems by our analysis to be possible only if this condition is met.

3. Governing equations for weak currents in the presence of surface waves

We assume that the dominant motion is that due to a number of discrete irrotational gravity waves, each characterized by its amplitude a, wavenumber m and frequency σ. The water is assumed to be homogeneous and of infinite depth, so that for each wave

$$\sigma^2 = gm, \tag{2}$$

where g is the gravitational acceleration.

The velocity vector $\mathbf{q}$ is then assumed to be of the form

$$\mathbf{q} = \epsilon\mathbf{u}_w + \epsilon^2\mathbf{v}, \tag{3}$$

where $\mathbf{u}_w$ represents the velocity attributable to the irrotational linearized solution for small amplitude gravity waves and $\mathbf{v}$ represents a perturbation of higher order. The small parameter ϵ may be regarded as characteristic of the wave slope; that is to say, it is $O(am)$ when a and m are the amplitude and wavenumber of a typical wave component. Note that $\mathbf{v}$ accounts both for currents and for higher-order corrections to $\mathbf{u}_w$ and therefore comprises both irrotational and rotational parts.‡

In accordance with earlier remarks, we assume a constant eddy viscosity of the form (1). Thus the vorticity equation is

$$\boldsymbol{\omega}_t = \operatorname{curl}(\mathbf{q}\times\boldsymbol{\omega}) + \nu_e\nabla^2\boldsymbol{\omega}, \tag{4}$$

where $\boldsymbol{\omega} = \operatorname{curl}\mathbf{q}$. Since

$$\mathbf{u}_w = \nabla\phi, \quad \nabla^2\phi = 0, \tag{5}$$

it follows that

$$\boldsymbol{\omega} = \epsilon^2 \operatorname{curl}\mathbf{v},$$

and we write

$$\mathbf{v} = \mathbf{v}_0 + \epsilon\mathbf{v}_1 + \ldots, \tag{6}$$

$$\operatorname{curl}\mathbf{v} = \boldsymbol{\omega}_0 + \epsilon\boldsymbol{\omega}_1 + \ldots. \tag{7}$$

† Ichiye (1967) has reported observations in the ocean consistent with the assumption of an eddy viscosity $\nu_e = O(\epsilon^2\lambda^2\sigma)$, where λ is the length of significant waves and σ is an average wave frequency. The same result for the eddy viscosity may be inferred from Phillips' (1963) theoretical estimate of the mean-square turbulent vorticity generated by wave motion. Phillips' estimate seems to remain valid in a mean flow possessing vorticity, providing the mean rotational rate of strain does not exceed that of the irrotational wave motion. Wave breaking is, however, not accounted for and (1) may not be appropriate if there is a significant amount of wave breaking.

‡ That the rotational and wave drift are both of order ϵ^2 times the phase velocity of the dominant waves in a wind-generated sea is confirmed by comparing a range of tabulated wave data with known empirical relations for the total surface drift. Bye (1967) has also stressed this point.

Each of the $\mathbf{v}_j$ and $\boldsymbol{\omega}_j$ may be separated into their mean and fluctuating components, denoted by $\overline{\mathbf{v}}_j$ and $\overline{\boldsymbol{\omega}}_j$, and $\langle \mathbf{v}_j \rangle$ and $\langle \boldsymbol{\omega}_j \rangle$, respectively, the mean being taken with respect to time. Since we are concerned only with solutions which are steady or periodic in time, quantities with an overbar are independent of time, and those in angular brackets are comprised of time-periodic components.

If one substitutes (6) and (7) into (4) and equates the coefficient of each power of ϵ to zero, a sequence of equations each of which may be separated into its mean and fluctuating parts is generated. The $O(\epsilon^2)$ equation is

$$\langle \boldsymbol{\omega}_0 \rangle_t = 0,$$

and, since $\langle \boldsymbol{\omega}_0 \rangle$ consists of periodic components, it follows that

$$\langle \boldsymbol{\omega}_0 \rangle = 0.$$

Accordingly, the next few equations are

$$\langle \boldsymbol{\omega}_1 \rangle_t = \operatorname{curl}(\mathbf{u}_w \times \overline{\boldsymbol{\omega}}_0), \tag{8}$$

$$0 = \operatorname{curl}(\overline{\mathbf{v}}_0 \times \overline{\boldsymbol{\omega}}_0) + \operatorname{curl}\overline{(\mathbf{u}_w \times \boldsymbol{\omega}_1)} + \alpha \nabla^2 \overline{\boldsymbol{\omega}}_0, \tag{9}$$

$$\langle \boldsymbol{\omega}_2 \rangle_t = \operatorname{curl}(\langle \mathbf{v}_0 \rangle \times \overline{\boldsymbol{\omega}}_0) + \operatorname{curl}\langle \mathbf{u}_w \times \boldsymbol{\omega}_1 \rangle.$$

From (8) and (9),

$$\langle \boldsymbol{\omega}_1 \rangle = \operatorname{curl}\left\{ \int^t \mathbf{u}_w dt \times \overline{\boldsymbol{\omega}}_0 \right\},$$

$$-\alpha \nabla^2 \overline{\boldsymbol{\omega}}_0 = \operatorname{curl}(\overline{\mathbf{v}}_0 \times \overline{\boldsymbol{\omega}}_0) + \operatorname{curl}\overline{(\mathbf{u}_w \times \langle \boldsymbol{\omega}_1 \rangle)}. \tag{10}$$

Using the fact that, by continuity,

$$\nabla . \mathbf{u}_w = \nabla^2 \phi = 0$$

vector identities yield

$$\langle \boldsymbol{\omega}_1 \rangle = (\overline{\boldsymbol{\omega}}_0 . \nabla) \int^t \mathbf{u}_w dt - \left(\int^t \mathbf{u}_w dt . \nabla \right) \overline{\boldsymbol{\omega}}_0,$$

$$\operatorname{curl}\overline{(\mathbf{u}_w \times \langle \boldsymbol{\omega}_1 \rangle)} = \overline{(\langle \boldsymbol{\omega}_1 \rangle . \nabla)\, \mathbf{u}_w} - \overline{(\mathbf{u}_w . \nabla) \langle \boldsymbol{\omega}_1 \rangle}.$$

On changing to Cartesian tensor notation, with a comma denoting partial differentiation, the last two results may be combined to yield

$$[\operatorname{curl}\overline{(\mathbf{u}_w \times \langle \boldsymbol{\omega}_1 \rangle)}]_i = \overline{\bar{\omega}_k^0 u_{i,j}^w \int^t u_{j,k}^w dt} - \overline{\bar{\omega}_{k,j}^0 u_{i,k}^w \int^t u_j^w dt}$$

$$+ \overline{u_k^w \left(\bar{\omega}_j^0 \int^t u_{i,j}^w dt \right)_{,k}} - \overline{u_k^w \left(\bar{\omega}_{i,j}^0 \int^t u_j^w dt \right)_{,k}}, \tag{11}$$

where $\bar{\omega}_i^0$ and u_i^w denote the ith components of $\overline{\boldsymbol{\omega}}_0$ and $\mathbf{u}_w$, respectively.

Now, the mean Lagrangian or Stokes drift $\mathbf{U}_s$ due to the irrotational motion (Phillips 1966, p. 31) has ith component

$$U_i^s = \overline{\epsilon^2 u_{i,j}^w \int^t u_j^w dt} \equiv \epsilon^2 u_i^s, \tag{12}$$

and (11) may be rearranged as

$$[\mathrm{curl}\,(\overline{\mathbf{u}_w \times \langle \boldsymbol{\omega}_1 \rangle})]_i = \bar{\omega}_k^0 u_{i,k}^s - \bar{\omega}_k^0 \overline{\frac{\partial}{\partial t}\left(\int^t u_j^w dt \int^t u_{i,jk}^w dt\right)}$$

$$- \bar{\omega}_{k,j}^0 \overline{\frac{\partial}{\partial t}\left(\int^t u_j^w dt \int^t u_{i,k}^w dt\right)} + \overline{u_k^w \left(\bar{\omega}_i^0 \int^t u_j^w dt\right)_{,jk}}. \quad (13a)$$

The final term on the right-hand side may be shown to equal

$$-\bar{\omega}_{i,k}^0 u_k^s + \frac{1}{2}\left[\bar{\omega}_i^0 \overline{\frac{\partial}{\partial t}\left(\int^t u_k^w dt \int^t u_j^w dt\right)}\right]_{,jk} - \frac{1}{2}\left[\bar{\omega}_i^0 \overline{\frac{\partial}{\partial t}\left(\int^t u_{k,j}^w dt \int^t u_{j,k}^w dt\right)}\right],$$

and since the mean of all time derivatives is zero, it follows that

$$\mathrm{curl}\,(\overline{\mathbf{u}_w \times \langle \boldsymbol{\omega}_1 \rangle}) = (\bar{\boldsymbol{\omega}}_0 . \nabla)\,\mathbf{u}_s - (\mathbf{u}_s . \nabla)\,\bar{\boldsymbol{\omega}}_0, \quad (13b)$$

where $\epsilon^2 \mathbf{u}_s = \mathbf{U}_s$.

Equation (10) for $\bar{\boldsymbol{\omega}}_0$ therefore becomes

$$-\alpha \nabla^2 \bar{\boldsymbol{\omega}}_0 = (\bar{\boldsymbol{\omega}}_0 . \nabla)\,(\bar{\mathbf{v}}_0 + \mathbf{u}_s) - (\bar{\mathbf{v}}_0 + \mathbf{u}_s) . \nabla \bar{\boldsymbol{\omega}}_0. \quad (14)$$

Now, if the assemblage of gravity waves is such that the Stokes drift may be taken as unidirectional (and consequently uniform in that direction, since $\nabla . \mathbf{U}_s = 0$), we may choose co-ordinates (x, y, z) such that

$$\mathbf{u}_s = [u_s(y, z), 0, 0], \quad \bar{\mathbf{v}}_0 = (u, v, w), \quad \bar{\boldsymbol{\omega}}_0 = \nabla \times \bar{\mathbf{v}}_0 = (\xi, \eta, \zeta),$$

z being measured vertically upwards from the mean free surface.

If we further restrict attention to solutions such that $\bar{\boldsymbol{\omega}}_0$ and $\bar{\mathbf{v}}_0$ are independent of x, the x component of (14) simplifies to

$$\alpha \nabla^2 \xi + \eta \frac{\partial u_s}{\partial y} + \zeta \frac{\partial u_s}{\partial z} = v \frac{\partial \xi}{\partial y} + w \frac{\partial \xi}{\partial z}, \quad (15)$$

$$\nabla^2 \equiv \partial^2/\partial y^2 + \partial^2/\partial z^2.$$

Notice that the contribution $\boldsymbol{\omega}_0 . \nabla \mathbf{v}_0$ vanishes identically because of the x independence. This equation expresses a balance between diffusion and convection of x vorticity and its renewal by vortex-line deformation through the action of the Stokes drift. In contrast, the other two component equations are not affected by the Stokes drift.

The averaged x momentum equation may be derived either directly from the Navier–Stokes equations or by integrating the y and z vorticity equations. This equation is

$$\alpha \nabla^2 u = v u_y + w u_z. \quad (16)$$

Equations (15) and (16) and the continuity equation

$$\partial v/\partial y + \partial w/\partial z = 0$$

govern the motion.

A stream function in the cross (y, z) plane may be defined such that

$$v = \partial \psi/\partial z, \quad w = -\partial \psi/\partial y,$$

in terms of which the equations reduce to

$$\alpha\nabla^4\psi + \frac{\partial(u, u_s)}{\partial(y, z)} = \frac{\partial(\nabla^2\psi, \psi)}{\partial(y, z)}, \tag{17}$$

$$\alpha\nabla^2 u = \partial(u, \psi)/\partial(y, z). \tag{18}$$

The kinematic boundary condition at the free surface $z = \epsilon z_1(x, y, t)$ yields the following boundary condition for the $O(\epsilon^2)$ mean flow:

$$w(y, 0) = \overline{-z_1\phi_{zz}} + (\overline{\phi_x z_{1,x} + \phi_y z_{1,y}}), \tag{19}$$

where

$$z_1 = \int^t \phi_z dt, \tag{19a}$$

the right-hand sides being evaluated at $z = 0$ and the subscripts x, y and z denoting partial differentiation. Hence

$$w(y, 0) = \frac{\partial}{\partial x}\overline{\left[\phi_x \int^t \phi_z dt\right]} + \frac{\partial}{\partial y}\overline{\left[\phi_y \int^t \phi_z dt\right]} \quad (z = 0). \tag{20}$$

Now, for an aggregate of plane gravity waves, ϕ is of the form

$$\phi = \mathrm{Re}\sum_\sigma e^{-i\sigma t} e^{mz} f(x, y, \sigma) \quad (m = \sigma^2/g), \tag{21}$$

and substitution of such a ϕ reveals that the right-hand side of (20) is

$$-\mathrm{Re}\sum_\sigma \frac{im}{2\sigma}(f_{xx} + f_{yy})f^*,$$

where * denotes the complex conjugate. Since $f_{xx} + f_{yy} = -m^2 f$, the appropriate boundary condition is simply

$$w(y, 0) = 0 \quad \text{or} \quad \psi(y, 0) = 0. \tag{22}$$

The boundary conditions at great depth are

$$u \to 0, \quad \psi \to 0 \quad (z \to -\infty). \tag{23}$$

We shall assume that appropriate stress conditions for the mean flow are that the mean (wind) stress is constant on the plane $z = 0$ and that the component of mean shear stress transverse to the wind direction vanishes on $z = 0$. That is,

$$\left.\begin{aligned} \nu_e \partial u/\partial z = \tau_w \quad \text{(constant)} \qquad & (24a) \\ \psi_{yy} - \psi_{zz} = 0 \qquad & (24b) \end{aligned}\right\} \quad (z = 0).$$

In view of (22), (24*b*) may be replaced by

$$\psi_{zz} = 0. \tag{24c}$$

In fact, (24*a*, *c*) may only be approximately true, for the precise tangential stress conditions depend on the variable stresses exerted by the wind on the free surface and also on the possible presence of surface contamination. If such stresses are neglected and if the gravity waves are adequately described as irrotational near the free surface, the *exact* $O(\epsilon^2)$ boundary condition for ψ is

$$\psi_{zz} - \psi_{yy} = -\overline{2z_1\phi_{yzz}} \quad (z = 0) \tag{25}$$

and substitution from (19a) and (21) yields

$$\psi_{zz} - \psi_{yy} = \mathrm{Re} \sum_{\sigma} \frac{-im^3}{\sigma} f f_y^* \quad (z = 0). \tag{26}$$

For the cases considered later, the right-hand side of (26) is zero. Actually, (17), (20) and (22) may themselves be inappropriate very close to the free surface; for there the influence of viscosity on the gravity waves may be significant (particularly if surface contamination is present). To deal with this, it would be necessary to develop a suitably matched 'inner solution' valid near $z = \epsilon z_1$. In addition, the right-hand side of (26) would be correspondingly modified. It is possible that the effect of viscosity on the waves could contribute an additional $O(\epsilon^2)$ mean flow. This is known to occur (see Phillips 1966, p. 38) in the case of wave attenuation by viscosity in the absence of wind. However, the calculation of such a flow is not pursued here.

We conclude this section by introducing dimensionless variables as follows:

$$u_s = c\hat{u}_s, \quad u = c\hat{u}, \quad \psi = cm_c^{-1}\hat{\psi}, \tag{27a–c}$$

$$(y, z) = m_c^{-1}(\hat{y}, \hat{z}), \quad R = c/\alpha m_c. \tag{27d, e}$$

The quantity R is ϵ^2 times the wave Reynolds number based upon the eddy viscosity ν_e and a characteristic wave speed c and wavenumber m_c. For definiteness, we take $\epsilon = am_c$, where a is a characteristic wave amplitude. In terms of the dimensionless (hatted) variables, our problem is

$$R^{-1}\hat{\nabla}^4\hat{\psi} + \frac{\partial(\hat{u}, \hat{u}_s)}{\partial(\hat{y}, \hat{z})} = \frac{\partial(\hat{\nabla}^2\hat{\psi}, \hat{\psi})}{\partial(\hat{y}, \hat{z})}, \tag{28}$$

$$R^{-1}\hat{\nabla}^2\hat{u} = \partial(\hat{u}, \hat{\psi})/\partial(\hat{y}, \hat{z}), \tag{29}$$

with boundary conditions

$$\frac{\partial\hat{u}}{\partial\hat{z}}(\hat{y}, 0) = \frac{u_*^2}{c^2}\frac{R}{\epsilon^4}, \tag{30a}$$

$$\hat{\psi}_{\hat{z}\hat{z}}(\hat{y}, 0) = 0, \quad \hat{\psi}(\hat{y}, 0) = 0 \tag{30b, c}$$

and

$$\hat{u} \to 0, \quad \hat{\psi} \to 0 \quad (\text{as } z \to \infty), \tag{30d, e}$$

where u_* is the water's friction velocity (such that the dimensional wind stress is $\tau_w = \rho u_*^2$, ρ being the water density).

We shall now dispense with the carets, and henceforth assume unless otherwise stated that all quantities have been made dimensionless as indicated.

4. Finite amplitude cells driven by monochromatic waves

In order to complete the statement of the mathematical problem, boundary conditions on two boundaries y = constant must be imposed. The Stokes drift, and therefore $u_s(y, z)$, is known since the irrotational wave field is assumed to be prescribed. If the Stokes drift is periodic in y, it is natural to impose the condition that the flow be periodic in y with the same period as $u_s(y, z)$. In these circumstances, (28) and (29) may be solved in principle, subject to the boundary conditions (30). The result produces the mean $O(\epsilon^2)$ currents associated with an

aggregate of plane waves yielding a periodic drift. In this section, a method of solution is formulated for a wave field consisting of a single pair of waves with equal amplitude a and dimensionless wavenumber vectors (k, l) and $(k, -l)$. Such waves are described by the dimensionless velocity potential

$$2e^z \cos ly \cos(kx - \sigma t), \quad k^2 + l^2 = 1.$$

The angle between the intersecting wave pairs is 2θ, so $k = \cos\theta$ and $l = \sin\theta$. For this wave field, the normalized Stokes drift is†

$$u_s = 2ke^{2z}[1 + k^2 \cos 2ly] \tag{31}$$

and is periodic in y.

It is natural to attempt to represent u and ψ by Fourier series in y:

$$\psi = \sum_{n=1}^{\infty} \phi_n(z) \sin 2lny, \tag{32}$$

$$u = U_h(z) + \sum_{n=1}^{\infty} u_n(z) \cos 2lny, \tag{33}$$

and it is also convenient to expand the x vorticity ξ in a similar fashion as

$$\xi = -\sum_{n=1}^{\infty} \xi_n(z) \sin 2lny. \tag{34}$$

The types of expansion are dictated by the fact that u is even in y while ψ is odd. The Fourier component in (33) that is independent of y has been denoted by $U_h(z)$ and is the horizontally averaged current.

If one substitutes (32)–(34) into the governing equations (28) and (29) and invokes the orthogonality of the Fourier components, the result is an infinite set of coupled ordinary differential equations for the coefficients $\phi_n(z)$, $\xi_n(z)$ and $u_n(z)$ $(n \geqslant 1)$ and the zeroth harmonic $U_h(z)$. The boundary conditions on these quantities are

$$\phi_n(0) = \xi_n(0) = u_n'(z) = 0 \quad (n \geqslant 1), \tag{35a–c}$$

$$U_h'(0) = u_*^2 R/\epsilon^4 c^2, \tag{35d}$$

where the primes denote d/dz. Notice that the wind stress imposes a condition only on $U_h(z)$.

A question exists as to whether the assumption of a constant eddy viscosity can lead to realistic profiles for $U_h(z)$. If nonlinear interactions are neglected, a constant eddy viscosity yields U_h' = constant, which is not realistic. It is possible that the feedback of higher harmonics will produce realistic results for $U_h(z)$ with the assumptions underlying this paper, but our resources did not permit us to explore the possibility. Instead, we assume U_h to result from an unspecified turbulent balance, and we do not require U_h to satisfy the stress relation (35d), which employs a constant eddy viscosity. (It is important to note at this point that, in a fluid of infinite depth, the existence of an applied stress at the surface leads to a linearly increasing (in time) total mean x momentum, and is therefore

† This was incorrectly given in Leibovich & Ulrich (1972), producing quantitative errors in that paper, but not affecting the conclusions drawn.

not consistent with a steady solution. Our procedure thus constructs a quasi-steady solution valid for a limited period of time.) 'Reasonable' forms for U_h are therefore asigned for the computations. A few numerical calculations have been carried out for $U_h'(z) =$ constant, but most of the work (and all that is reported here) has been carried out using an empirically observed current profile (to be introduced in § 7).

The equations for the quantities $\xi_n(z)$, $\phi_n(z)$ and $u_n(z)$ may be written as

$$\left.\begin{aligned} L_n\xi_n &= lRF_n, \quad L_n\phi_n = \xi_n, \quad L_n u_n = lRG_n, \\ L_n(\ ) &= d^2(\ )/dz^2 - 4n^2l^2(\ ), \end{aligned}\right\} \quad n = 1,2,\ldots, \tag{36}$$

$$\begin{aligned} F_n = 2e^{2z}[4knu_n + k^3(u'_{n+1} - u'_{n-1} + 2(n+1)u_{n+1} + 2(n-1)u_{n-1})] - \delta_{n1}4k^3e^{2z}U_h' \\ + \sum_{k=1}^{n-1} k(\xi_k\phi'_{n-k} - \phi_k\xi'_{n-k}) \\ + \sum_{k=1}^{\infty} [k(\xi_k\phi'_{n+k} - \phi_k\xi'_{n+k}) - (n+k)(\xi_{n+k}\phi'_k - \phi_{n+k}\xi'_k)], \end{aligned}$$

$$\begin{aligned} G_n = -2n\phi_n U_h' + \sum_{k=1}^{n-1} (k u_k\phi'_{n-k} - (n-k)u'_k\phi_{n-k}) \\ - \sum_{k=1}^{\infty} (k u_k\phi'_{n+k} + (n+k)\phi_{n+k}u'_k), \end{aligned}$$

$$\delta_{n1} = \begin{cases} 1, & n = 1, \\ 0, & n \neq 1, \end{cases}$$

$$\xi_n(0) = \phi_n(0) = u_n'(0) = \phi_n(-\infty) = \xi_n(-\infty) = U_h(-\infty) = 0.$$

Quantities with subscripts less than 1 are identically zero.

The solution to the problem

$$L_n\chi = f, \quad \chi(0) = \chi(-\infty) = 0, \tag{37}$$

where f is a known function which tends to zero as $z \to -\infty$, is

$$\chi = M_n(f), \tag{38}$$

where
$$M_n f = \frac{1}{2nl}\left[e^{2nlz}\int_z^0 f(\zeta)\sinh 2nl\zeta\, d\zeta + \sinh 2nlz \int_{-\infty}^z f e^{2nl\zeta}\, d\zeta\right], \tag{39}$$

and the solution to the problem

$$L_n\Omega = g, \quad \Omega'(0) = \Omega(-\infty) = 0, \tag{40}$$

where g is a known function tending to zero as $z \to -\infty$, is

$$\Omega = O_n(g),$$

where

$$O_n(g) = -\frac{1}{2nl}\left[\cosh 2nlz \int_{-\infty}^z g(\zeta)\, e^{2nl\zeta}\, d\zeta + e^{2nlz}\int_z^0 g(\zeta)\cosh 2nl\zeta\, d\zeta\right]. \tag{41}$$

We truncate the infinite set (36) by setting all ξ_n, ϕ_n and u_n with $n \geqslant N$ equal to zero. In our computations we have generally set $N = 3$, although we have taken $N = 5$ for some runs to check the accuracy of the procedure. After truncation, we are left with a set of $3N$ nonlinear equations.

To solve the truncated set, we convert (36) into the $6N$ integral equations by using the operators M_n and O_n:

$$\left.\begin{aligned} &\xi_n = RM_n(F_n[\xi_i, \phi_j, u_k, \xi'_\alpha, \phi'_\beta, u'_\gamma]), \quad \xi'_n = RM'_n(F_n), \\ &\phi_n = M_n(\xi_n), \quad \phi'_n = M'_n(\xi_n), \\ &u_n = RO_n(G_n[\xi_i, \phi_j, u_k, \xi'_\alpha, \phi'_\beta, u'_\gamma, U'_h, z]), \quad u'_n = RO'_n(G_n), \end{aligned}\right\} \tag{42}$$

where
$$M'_n(f) = e^{2nlz}\int_z^0 f(\zeta)\sinh 2nl\zeta\, d\zeta + \cosh 2nlz \int_{-\infty}^z f(\zeta)\, e^{2nl\zeta}\, d\zeta, \tag{43}$$

$$O'_n(g) = -\left(e^{2nlz}\int_z^0 g(\zeta)\cosh 2nl\zeta\, d\zeta + \sinh 2nlz \int_{-\infty}^z g(\zeta)\, e^{2nl\zeta}\, d\zeta\right), \tag{44}$$

and $n, i, j, k, \alpha, \beta, \gamma = 1, \ldots, N$. These equations are solved by making the initial choice $\xi_n = \xi'_n = \phi_n = \phi'_n = u_n = u'_n = 0$ for $n = 1, \ldots, N$.

New values of the $6N$ unknowns are found by carrying out the integration operations M_n, O_n, M'_n and O'_n in the sequence indicated in (42), always using the most recent data to evaluate the right-hand sides. More detail about the numerical treatment is provided in the appendix.

Convergence of the method for a given functional form for $U'_h(z)$ depends upon R and the parameter l ($= \sin\theta$, where 2θ is the angle between the crossed wave pair). We do not attempt to establish theoretical limits for the parametric domain of convergence of the procedure in this paper. Solutions obtained by this method will be described in § 7.

The next section describes a related solution procedure.

5. A perturbation solution

Wind waves are a random phenomenon, and the model of a wave field consisting of two crossed trains of regular waves obviously leaves many questions unanswered. One important matter is that of the spacing of LC cells. It seems likely that this can best be approached by statistical considerations. A statistical treatment incorporating the nonlinear equations (28) and (29) appears intractable. There may be cases, however, where (28) and (29) can be linearized without losing meaning, and such a linearization will make a statistical analysis feasible. The purpose of this section is to discuss the linearization, or more generally, the solution of (28) and (29) by perturbation, and the properties of the solutions so obtained.

We have formulated the problem such that all parts of the current system, including the averaged current U_h, the wave drift u_s and the Langmuir circulations, represented by ψ and $u - U_h$, may be of comparable intensity. There are some indications, however, that at least in some circumstances the dimensionless shear $U'_h(z)$ may be somewhat larger than u_s and the other components of the current (Masch 1963) and their gradients. If we take the parameter Λ as a measure of $U'_h(z)$, then (35d) provides an estimate of its magnitude:

$$\Lambda = O(u_*^2 R/\epsilon^4 c^2), \quad U'_h(z) = \Lambda \tilde{U}'_h(z), \tag{45}$$

where $\tilde{U}'_h$ is $O(1)$. We shall introduce Λ according to (45) with the order symbol replaced by equality.

An iterative procedure such as the one described in §4 produces a series solution of the form

$$\left.\begin{aligned} \psi(y,z) &= \Lambda R \sum_{n=0}^{\infty} (\Lambda R^2)^n \psi_n(y,z), \\ u(y,z) - U_h(z) &= (\Lambda R)^2 \sum_{n=0}^{\infty} (\Lambda R^2)^n U_n(y,z), \end{aligned}\right\} \tag{46}$$

where the first terms satisfy the equations

$$\nabla^4 \psi_0 = \bar{U}_h' \partial u_s/\partial y, \quad \nabla^2 U_0 = -\bar{U}_h' \partial \psi_0/\partial y. \tag{47}$$

Convergence of the iteration scheme previously described is therefore expected to be linked to the convergence of the series (46). For ΛR^2 small enough convergence is expected.

It may be verified that if (47) is specialized to constant $\bar{U}_h'$ and u_s, corresponding to a single wave pair, then (47) reduces to the equations used in Craik's (1970) viscous analysis. The validity of Craik's approximations may therefore be assessed by comparison. For the wave pair leading to the Stokes drift (31), the solutions for ψ_0 and U_0 are

$$\left.\begin{aligned} \psi_0 &= 4k^3 l \sin(2ly + \Delta)\, \chi_0(z), \quad \chi_0(z) = -M_1\{M_1(\bar{U}_h' e^{2z})\}, \\ U_0 &= 8k^3 l^2 \cos(2ly + \Delta)\, S(z), \quad S(z) = -O_1(\bar{U}_h' \chi), \end{aligned}\right\} \tag{48}$$

where M_1 and O_1 are defined by (39) and (41) and Δ is a phase factor determined by that of the waves (and may be omitted without loss of generality, as in (31), when only a single wave pair is considered).

For $\bar{U}_h' =$ constant, the solution (48) is given by Craik (1970, §6), and figure 6 of that paper illustrates the structure of the longitudinal vortices that emerge.

The functions $\chi_0(z)$ and $S(z)$ corresponding to $\bar{U}_h' = 1$ are recorded here for future reference (these results correct those found in §6 of Craik 1970):

$$\chi_0(z;l) = \frac{1}{16k^4}\left\{e^{2lz}\left(1 + \frac{k^2}{l} z\right) - e^{2z}\right\}, \tag{49}$$

$$S(z;l) = \frac{1}{16k^4}\left[\frac{1}{4k^2} e^{2z} - \frac{e^{2lz}}{8}\left(\frac{k^2}{l^2} z^2 + \frac{5l^2 - 1}{2l^3} z + \frac{5l^4 + 8l^3 - 6l^2 + 1}{4k^2 l^4}\right)\right], \tag{50}$$

and in particular

$$\chi_0'(0;l) = (1-l)^2/16k^4 l. \tag{51}$$

It is apparent from the definition (39) of M_1 that $f M_1(f) < 0$. Therefore the sign of $M_1\{M_1(f)\}$ is the same as that of f. Since $\bar{U}_h'$ is assumed to be positive, $\chi < 0$ as well. In a similar way, one sees from (41) that, with negative $\chi(z)$ and $\bar{U}_h'(z)$, $S(z) < 0$. Since the vertical velocity component is (to this approximation)

$$-8k^3 l^2 \Lambda R \chi(z) \cos(2ly + \Delta) \tag{52}$$

and the x velocity component is

$$U_0 = 8k^3 l^2 (\Lambda R)^2 S(z) \cos(2ly + \Delta) \tag{53}$$

positive vertical velocity (upwelling) is associated with negative U_0, according to this linearized solution for arbitrary (but positive) $\bar{U}_h'(z)$. This means that downward motions occur midway between lines of maximum wave height,

while upwelling occurs under these lines. Corresponding to this, the contribution U_0 to the downwind current due to the Langmuir cells is positive over downwelling (convergence) sites. This is the behaviour known for the total downwind surface drift, which is observed to be greatest over convergence lines and least between them. Thus, in order for the model accurately to reflect this aspect of observation, the LC contribution U_0 must be greater in magnitude than the periodic portion of the wave drift, which has the opposite behaviour. This point was made earlier by Leibovich & Ulrich (1972). The total downwind (dimensionless) surface drift is

$$U_h(0) + 2k + 2k^3(1 + 4l^2R^2\Lambda^2 S(0)) \cos(2ly + \Delta), \tag{54}$$

so that this condition requires that

$$\mathscr{S}_d \equiv 1 + 4l^2R^2\Lambda^2 S(0) < 0. \tag{55}$$

Our linearization procedure requires $R^2\Lambda$ to be small, but does not restrict the magnitude of ΛR. The former limitation does not apply for nonlinear (numerical) solutions to be discussed later. We note at this point, however, that there is fair agreement between the nonlinear computer results and solutions of (47) in parameter ranges for which $\mathscr{S}_d < 0$.

We may estimate Λ and R, and thus assess the circumstances in which $\mathscr{S}_d$ may be expected to be negative and also those conditions under which the solution procedures discussed in this paper may be valid. From its definition, $R = c/\alpha m$, and expressing α in terms of the eddy viscosity ν_e,

$$R = c\epsilon^2/\nu_e m, \tag{56}$$

and from (45)
$$\Lambda = \frac{u_2^* R}{\epsilon^4 c^2} = \frac{u_*^2}{\epsilon^2 c^2}\left(\frac{c}{\nu_e m}\right),$$

so
$$\Lambda R = \left(\frac{u_*}{c}\right)^2 \left(\frac{c}{\nu_e m}\right)^2, \quad \Lambda R^2 = \left(\frac{u_*}{c}\right)^2 \left(\frac{c}{\nu_e m}\right)^3 \epsilon^2. \tag{57), (58}$$

Estimates of (57) and (58) may be made by observing that $U_* \approx \gamma U_{\text{surf}}$, where commonly $\frac{1}{25} < \gamma < \frac{1}{22}$ (cf. Bye 1965), and U_{surf}, the surface water current, is known to be about $0{\cdot}033W$ (see, for example, Keulegan (1951) or Hidy & Plate (1966) for results in laboratory channels and Bye (1965) for lakes), where W is the wind speed. Thus $U_* = O(10^{-3}W)$, and we may estimate (57) and (58) to be

$$\Lambda R = O\left[10^{-6}\left(\frac{W}{\nu_e m}\right)^2\right], \quad \Lambda R^2 = O\left[10^{-6}\frac{c}{W}\left(\frac{W}{\nu_e m}\right)^3 \epsilon^2\right]. \tag{57a), (58a)}$$

For a 'fully developed sea' we may further estimate (Stewart 1967) $c \doteqdot W$ and $m \doteqdot g/W^2$, so for this case $\Lambda R = O[10^{-6}(W^3/g\nu_e)^2]$ and $\Lambda R^2 = O[10^{-6}(W^3/\nu_e g)^3 \epsilon^2]$. If ΛR is to be $O(1)$ (to establish the condition (55)), then $W^3/g\nu_e = O(10^3)$, and so $\Lambda R^2 = O(10^3\epsilon^2)$, or $\epsilon \ll 0{\cdot}03$. This condition on the wave slope is unrealistically severe; in fact, as indicated by Longuet-Higgins (1969, p. 157), for a 'fully developed sea' the wave amplitude may be estimated to be about $\frac{1}{8}W^2/g$, so that, with $m = g/W^2$, $\epsilon = am \doteqdot \frac{1}{8}$, independent of W.

For a fetch-limited situation, $c/W < 1$; thus ΛR will be $O(1)$ for $W/\nu_e m = O(10^3)$, yielding $\Lambda R^2 = O(10^3 \epsilon^2 c/W)$. This situation is only slightly better than that for the fully developed sea (particularly since we expect $\epsilon > \frac{1}{8}$ for the fetch-limited case). Nevertheless, it is possible that the first term of the ΛR^2 series, which is a good approximation for sufficiently small ϵ, may continue to describe the basic characteristics of solutions for larger ϵ, although it is no longer a formally valid approximation.

6. Motions driven by waves with a discrete symmetric spectrum: the predicted spacing

Here we revert to dimensional variables. The solutions discussed so far relate only to a single pair of waves with periodicities of the form $\exp i(kx \pm ly - mct)$. These waves are of equal amplitude and propagate at equal and opposite angles to the wind direction. One may represent a complete directional gravity-wave field symmetric about the wind direction as the sum of a large number of such (discrete) wave pairs. Assume, then, that the wave field has the form $\epsilon \mathbf{u}_w = \nabla\Phi$, where Φ is the (dimensional) wave velocity potential

$$\Phi = \sum_{j=1}^{N} A_j \exp(m_j z)\{\cos(k_j x + l_j y - \sigma_j t + \Delta_{1j}) + \cos(k_j x - l_j y - \sigma_j t + \Delta_{2j})\},$$

$$m_j^2 = k_j^2 + l_j^2, \quad \sigma_j^2 = g m_j,$$

where $A_j = \sigma_j a_j / m_j$, with a_j the amplitude of a plane wave, and Δ_{1j} and Δ_{2j} are random phases.

For this collection of plane waves, the drift, defined as the time average

$$(\mathbf{U}_s)_i = \lim_{T\to\infty} \frac{1}{T} \int_0^T \left[\int^t \Phi_{,j}\, dt\, \Phi_{,ij} \right] dt,$$

will yield a Stokes drift that is unidirectional and independent of x provided that the set of frequencies $\{\sigma_j\}$ are distinct. We shall assume that the spectrum satisfies this requirement (if it does not $\mathbf{U}_s$ is periodic in x, and has a vertical as well as a horizontal component). Then $\mathbf{U}_s$ has only an x component U_s given by

$$U_s = \sum_{j=1}^{N} 2a_j^2 k_j \sigma_j \exp(2m_j z)\left[1 + \frac{k_j^2}{m_j^2}\cos(2l_j y + \delta_j)\right], \tag{59}$$

where $\delta_j = \Delta_{1j} - \Delta_{2j}$. The drift in this case is the sum of the drifts due to each wave pair.

For such a wave field, it is of particular interest to discover whether a dominant spanwise spacing of the circulations is likely to emerge. This will clearly be so if the wave field is dominated by a few very prominent wave pairs. It is probably only in this situation that extremely regular and parallel streaks will be observed (see, for example, the photographs of Stommel 1951). In such cases, the spacing of windrows should be just half the spanwise wavelength of the dominant waves (i.e. equal to π/l).

More often, the windrow pattern is rather irregular but still displays a characteristic spanwise spacing. Here, individual wave pairs are unlikely to dominate

the wave field, but estimates of the characteristic spacing can still be made. A first attempt by Craik (1970, § 8), for a simple directional wave spectrum and a linear mean velocity profile, led to the prediction that the row spacing should normally be approximately equal to the cut-off wavelength λ_0 of the (continuous) wave-energy spectrum. This prediction identified the preferred spacing with the wavelength of that Fourier component (in y) of the secondary current system which had greatest longitudinal vorticity. In fact, correction of a numerical error yields a revised spacing of $1{\cdot}67\lambda_0$.

However, the *ad hoc* nature of the spacing criterion used is unsatisfactory, and furthermore the basis of this estimate is suspect. Indeed, it is inappropriate to represent the wave field by a continuous wavenumber spectrum in our model because the random phase associated with each Fourier component of the periodic wave drift causes this current system to phase mix to zero. More precisely, for a continuous wave spectrum of *finite* total energy, a statistical formulation of the secondary current system has zero variance and hence no spanwise structure. In physical terms, if a *fixed* amount of wave energy is distributed between N discrete wave pairs, the Stokes drift becomes more nearly uniform as N is increased; in the limit $N \to \infty$ no distortion of spanwise-oriented vortex lines occurs and no longitudinal vorticity is created. Consequently, the existence of secondary flows of the kind in view requires concentration of a finite amount of wave energy in *discrete* wave pairs (which correspond to delta functions of a continuous spectrum). The number of such discrete waves may of course be large.

We assume that ΛR^2 is sufficiently small to allow description of the motion by the linearized analysis of the last section. On considering the N discrete wave pairs to have random phases uniformly distributed in $[0, 2\pi]$, the LC stream function is given approximately by

$$\psi = R\Lambda \operatorname{Re} \sum_{j=1}^{N} \Gamma_j(z) \exp\left\{i\left[2\frac{l_j}{m_j}y - \frac{\pi}{2} + \delta_j\right]\right\},$$

$$\Gamma_j \equiv 4a_j^2 \sigma_j k_j^3 l_j m_j^{-4} \chi_j(m_j z; l_j),$$

$$l_j^2 + k_j^2 = m_j^2, \quad R = c/\alpha m_0,$$

where each (real) χ_j is given by a result equivalent to that for χ_0 in (48), approximately, and c and m_0 are a characteristic wave speed and wavenumber. The statistical properties of such random functions, for N large, have been examined by Rice (1944) and Longuet-Higgins (1962) and yield an alternative estimate of the preferred spacing.

The spanwise velocity component $v(y, 0) = \partial\psi(y, 0)/\partial z$ at the free surface has two kinds of zero; one corresponding to a diverging surface flow and upwelling, the other to a converging surface flow and downwelling. Windrows are normally located at zeros of $v(y, 0)$ of the latter kind, and are therefore associated with just half the zeros of $v(y, 0)$.

The correlation function $\Psi(y)$ for $v(y, 0)$ is

$$\Psi(y) \equiv \overline{v(y', 0)\, v(y' + y, 0)} = (\Lambda R)^2 \sum_{j=1}^{N} \Gamma_j'^2(0, l_j) \cos 2l_j y, \tag{60}$$

where $\Gamma_j' \equiv d\Gamma_j/dz$ and the bar denotes the average with respect to y'. Also (see Longuet-Higgins 1962, §2) the energy spectrum $E(l)$ is

$$E(l) = \frac{1}{\pi}\int_0^\infty \Psi(y)\cos 2ly\,dy,$$

the moments m_r are defined as

$$m_r = 2^{r+1}\int_0^\infty E(l)\,l^r\,dl$$

and, when r is even,

$$m_r = (-1)^{\frac{1}{2}r}(d^r\Psi/dy^r)_{y=0}.$$

Now we suppose that each component of $v(y, 0)$ has finite energy (or dispersion), so that the total energy increases uniformly with N. Formally, we shall consider the energy to increase without bound as $N\to\infty$, though in practice we must restrict N to be large but finite. Also, in the limit $N\to\infty$, the energy of each component is a vanishingly small fraction of the total energy. In such circumstances, the central limit theorem holds for $v(y, 0)$ (see Cramér 1937, p. 56) and the mean number of zeros of $v(y, 0)$ per unit distance in the y direction is (Longuet-Higgins 1962, equation 2.4.2)

$$Q = \frac{1}{\pi}\left(\frac{m_2}{m_0}\right)^{\frac{1}{2}} = \frac{1}{\pi}\left(-\frac{d^2\Psi}{dy^2}\Big/\Psi\right)_{y=0}^{\frac{1}{2}}.$$

From (60),
$$Q = \lim_{N\to\infty}\frac{2}{\pi}\left\{\sum_{j=1}^N l_j^2\Gamma_j'^2(0, l_j)\right\}^{\frac{1}{2}}\left\{\sum_{j=1}^N \Gamma_j'^2(0, l_j)\right\}^{-\frac{1}{2}}. \tag{61}$$

The expected number of windrows per unit distance in the y direction is therefore $\frac{1}{2}Q$.

To test this estimate, we now examine a particular set of wave pairs. For simplicity, the wavenumber $m_j = (k_j^2 + l_j^2)^{\frac{1}{2}}$ of each pair is considered to lie within a narrow band centred on the value m_0 (but each m_j is assumed to be different, ensuring that each pair has a different frequency). The amplitude a_j and directional wavenumbers $(k_j, \pm l_j)$ of each pair are chosen to satisfy

$$a_j^2 = a_0^2\cos^2\theta_j, \quad \theta_j = j\pi/N \quad (j = 1, 2, \ldots, N),$$

where $\pm\theta_j$ are the angles of propagation relative to the wind direction of each wave train so $l_j = m_j\sin\theta_j$, etc. Here a_0 is a characteristic amplitude, the wave-slope parameter ϵ is defined as $a_0 m_0$ and the velocity scale c is taken as $(g/m_0)^{\frac{1}{2}}$ to a good approximation. To avoid undue complications in evaluating the functions Γ_j' from (48), it is further assumed that U_h' is constant, so that Γ_j may be found from (51), or since $m_j \approx m_0$ and $\sigma_j \approx (g/m_0)^{\frac{1}{2}}$,

$$\Gamma_j'(0) = \tfrac{1}{4}a_0^2\left(\frac{g}{m_0}\right)^{\frac{1}{2}}\frac{k_j(m_0 - l_j)^2}{m_0^2}.$$

Thus
$$Q = \lim_{N\to\infty}\frac{2m_0}{\pi}\left[\frac{\sum_{j=1}^N \cos^2\theta_j\sin^2\theta_j(1-\sin\theta_j)^4}{\sum_{j=1}^N \cos^2\theta_j(1-\sin\theta_j)^4}\right]^{\frac{1}{2}},$$

and we may replace the sums by integrals over θ in the limit, so that

$$Q = \frac{2m_0}{\pi}\left[\frac{\int_0^{\frac{1}{2}\pi}\cos^2\theta\sin^4\theta(1-\sin\theta)^4\,d\theta}{\int_0^{\frac{1}{2}\pi}\cos^2\theta\sin^2\theta(1-\sin\theta)^4\,d\theta}\right]^{\frac{1}{2}}$$

$$= \frac{2m_0}{\pi}\left(\frac{J_1}{J_2}\right)^{\frac{1}{2}}.$$

The integrals J_1 and J_2 may be evaluated to yield

$$Q = \frac{2m_0}{\pi}\left[\frac{\frac{69}{256}\pi - \frac{88}{105}}{\frac{21}{32}\pi - \frac{28}{15}}\right]^{\frac{1}{2}} = \frac{2m_0}{\pi}(0{\cdot}2108).$$

The expected number of windrows per unit distance in the y direction is $\frac{1}{2}Q$, and the inverse of this is the expected distance between windrows. If we denote this distance by D_w, then

$$D_w = \pi/(0{\cdot}2108m_0) = 2{\cdot}372\lambda, \tag{62}$$

where $\lambda = 2\pi/m_0$ is the characteristic wavelength of the wave field. This may be compared with the cruder (corrected) estimate $D_w = 1{\cdot}67\lambda$ given by Craik's (1970) criterion. It is perhaps worth noting that the spacing (62) would occur for a *single* wave pair with a propagation angle of $\pm 12{\cdot}2°$ to the wind direction. The directional spectrum $a_j^2 = a_0^2\cos^{\frac{3}{2}}\theta_j$ yields $D_w = 2{\cdot}29\lambda$; this suggests that the spacing may not be highly sensitive to the directional properties of the spectrum.

7. Numerical results

Our purpose in pursuing the numerical computations to be described here was to discover the extent to which the general features LC (1)–(5) are produced by our model. Since LC (1) and LC (2) are automatic consequences of the model, we focus upon LC (3)–(5). We have *not* undertaken a complete numerical study of the model equations (28) and (29), but have restricted ourselves to the solution method described in § 4, and to special choices of R and $U_h'(z)$.

The computation requires selection of the parameter R, which in turn requires the eddy viscosity to be chosen. To simplify the choice of parameters, and yet still strive for realism, we have tried where possible to relate the required empirical constants occurring in the model to the wind speed.

The choice of a value for the eddy viscosity poses problems, since measured eddy viscosities include the effects of the Langmuir circulations themselves. We should like to separate out the contribution of turbulence scales smaller than the LC's and assign an eddy viscosity representing only their effects. There is no recognized way to accomplish this, so for our numerical experiments, we have adopted the classical correlation due to Ekman (cf. Sverdrup, Johnson & Fleming 1942) for the vertical eddy viscosity:

$$\nu_e = 4{\cdot}3\times 10^{-4}W^2\ \mathrm{s}, \tag{63}$$

where W is the wind speed (at a few metres above the water surface). This formula, proposed for wind speeds exceeding 6 m/s but used here for all W, is based upon observations of ocean currents and must include the mixing effect of LC's. In adopting (63), it is but small comfort to realize that the fact that LC contributions should be removed is partly balanced by the likelihood that wave breaking near the surface must be underestimated by (63).

With (63), $R = c\epsilon^2/\nu_e m = (c\epsilon^2 \times 10^4/4{\cdot}3W^2 m)\ \mathrm{s}^{-1}$. In this expression, and those to follow, we put $c = W$ and $m = g/W^2$ in order to reduce the number of independent input parameters. (These choices correspond to a 'fully developed sea'.) With this done,

$$R = \frac{\epsilon^2 \times 10^4}{4{\cdot}3}\frac{W}{g}\,\mathrm{s}^{-1}, \tag{64}$$

so that R is fixed by the specification of ϵ and $(W/g)\ \mathrm{s}^{-1}$.

The logarithmic profile observed by Bye (1965) is used for $U_h'(z)$. In dimensional variables, Bye's profile is

$$U_{\text{current}}(z) = U_{\text{surf.}} - \frac{U_*}{k}\ln\frac{z}{z_0}, \quad z \leqslant z_0 < 0,$$

where $U_{\text{surf.}}$ is the water surface speed, U_* is the friction velocity, $k = 0{\cdot}4$ is von Kármán's constant and z_0 is a roughness length. We take $U_{\text{surf.}} = 0{\cdot}033W$ and $U_*/U_{\text{surf.}} = \frac{1}{22}$ as indicated earlier. Only the shear U_h' appears in our problem, and so the roughness length z_0 is not explicitly required. We have implicitly taken z_0 to be less than one mesh unit since our numerical computation uses the following form for the shear U_h' (now in dimensionless variables):

$$U_h'(z): \begin{cases} 0{\cdot}00375/\epsilon^2|z|, & |z| \geqslant h, \\ 0{\cdot}00375/\epsilon^2 h, & z = 0, \end{cases} \tag{65}$$

where h is the mesh length in the z direction. Since we have taken $h = 0{\cdot}05$, $z = -h$ corresponds to $7{\cdot}96 \times 10^{-3}$ times the wavelength of the surface waves. Using the empirical correlations already discussed, and standard empirical results for the length of fully developed wind waves, one can show that the roughness length calculated from Ellison's (1956, p. 409) data is considerably smaller than h.

Thus, with (64) and (65), the numerical problem is specified by the specification of ϵ, W/g s ($\equiv WG$, say) and the propagation angle θ of the intersecting wave trains. (Note that $WG = 0{\cdot}1$, for example, corresponds to a wind speed of 0·98 m/s.)

One (convergent) calculation was carried out for $U_h' = \text{constant} = 1$ and $R = 2$. Only selected results computed with (64) and (65) will be presented here. In most cases, (36) were truncated at $N = 3$ (so that only the first three harmonics were computed). A few runs allowing for five harmonics were carried out to check the convergence of the procedure (in N). These calculations were done for $\theta = 24°$, $\epsilon = 0{\cdot}05$ and $R = 0{\cdot}29$, $0{\cdot}58$, $0{\cdot}87$, $1{\cdot}16$ and $1{\cdot}45$, and the first three harmonics were compared with the corresponding results for $N = 3$. Agreement was within 4 % in all cases and improved as R decreased. The case $R = 1{\cdot}74$

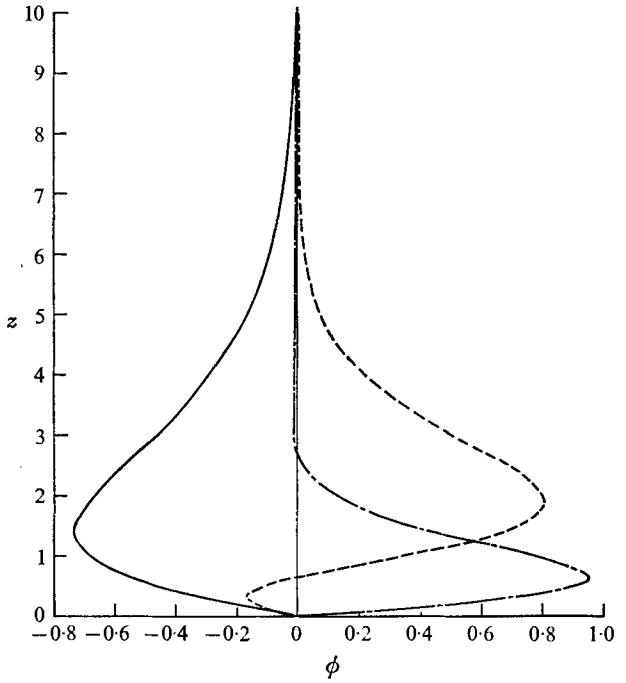

FIGURE 1. Fourier coefficients ϕ_1, ϕ_2 and ϕ_3 as functions of z for the case of a wave angle $\theta = 24°$, wave-slope parameter $\epsilon = 0{\cdot}05$ and wind-speed parameter $WG \equiv (W/g)\,\mathrm{s} = 0{\cdot}25$. ——, ϕ_1; – – –, $\phi_2 \times 10^2$; — · —, $\phi_3 \times 10^3$.

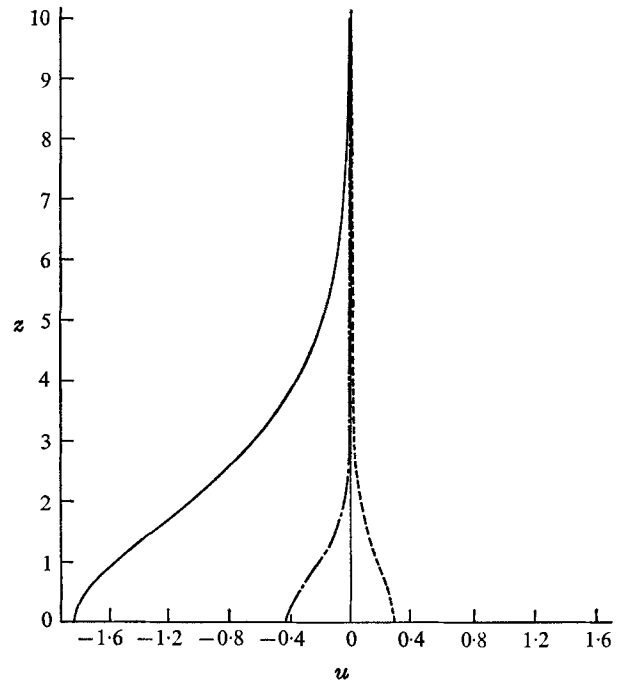

FIGURE 2. Fourier coefficients u_1, u_2 and u_3 for the case shown in figure 1. ——, u_1; – – –, u_2; — · —, $u_3 \times 10$.

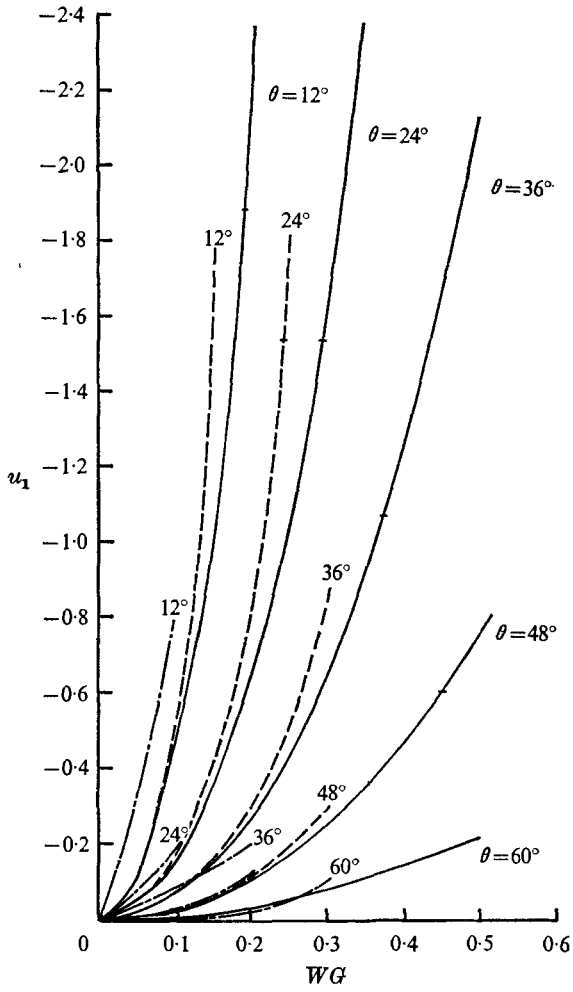

FIGURE 3. Surface value of the first harmonic u_1 of the Langmuir circulation's contribution to the wind-directed drift as function of θ, ϵ and WG. Tick marks indicate conditions at which the sum of $u_1(0)$ and the surface value of the Stokes wave drift vanishes. ——, $\epsilon = 0{\cdot}025$; – – –, $\epsilon = 0{\cdot}05$; — · —, $\epsilon = 0{\cdot}075$.

was also computed, but the iterations failed to converge (see appendix for convergence criterion) for both $N = 3$ and $N = 5$. For $N = 3$, it was found that, if the iterations diverged for a given R, ϵ and θ, then they would also diverge if R, ϵ and $\alpha = \frac{1}{2}\pi - \theta$ were increased, but might converge upon reduction of one or all of the parameters R, ϵ and α.

Typical results for the Fourier coefficients ϕ_n and u_n ($n = 1, 2, 3$) are given in figures 1 and 2. The case illustrated is $\theta = 24°$, $\epsilon = 0{\cdot}05$ and W/g s $= 0{\cdot}25$. A feature to note is that near the surface ϕ_1 and ϕ_2 are both negative, which implies that the downwelling is enhanced and upwelling is retarded. Although this tendency is small (since ϕ_2 is small compared with ϕ_1), the consequent asymmetry between upwelling and downwelling corresponds to observed circulation patterns

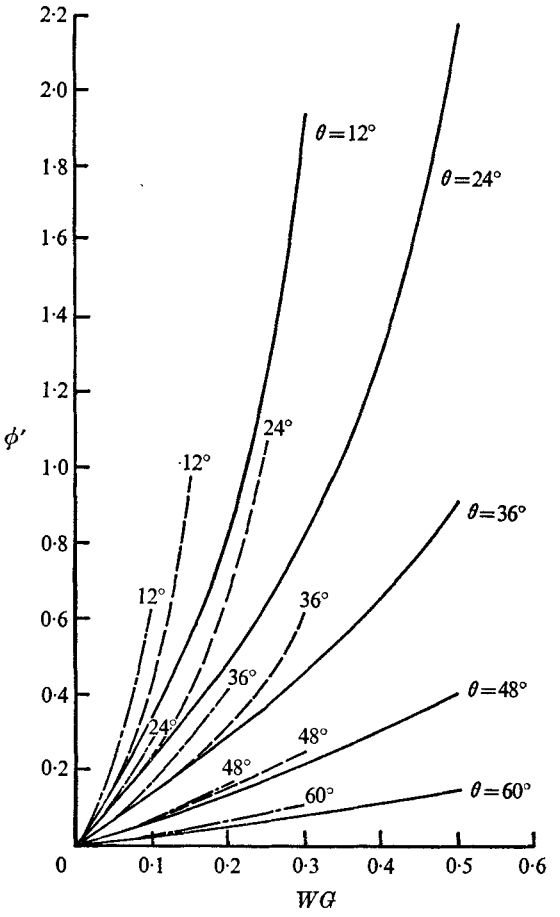

FIGURE 4. Surface values of $\phi_1'(0)$, the peak surface value of the first harmonic of the spanwise velocity component in the circulation cell, as a function of θ, ϵ and WG. ——, $\epsilon = 0{\cdot}025$; – – –, $\epsilon = 0{\cdot}05$; — · —, $\epsilon = 0{\cdot}075$.

(see, for example, Myer 1971). Another significant feature in figure 2 is that the surface value of u_1 opposes the periodic portion of the wave drift, and the quantity $\mathscr{S}_d$ introduced in (55) is negative. Therefore, for this case, downwelling takes place below lines where the wind-directed surface current is greatest. Thus the two LC features LC (3) and LC (4) of § 2 are possible consequences of our model.

Figure 3 presents $u_1(0)$, the first harmonic of the LC contribution to the wind-directed surface drift, as a function of WG, θ and ϵ. Each curve ends either at $WG = 0{\cdot}5$ or the greatest value of WG for which the iterations converged if this is less than 0·5. Tick marks, where they occur, represent $2\cos^3\theta$, which is the magnitude of the maximum periodic part of the wave drift. Therefore, on curves thus marked, the quantity $\mathscr{S}_d$ defined in (55) is negative for WG exceeding its value at the mark.

Figure 4 presents $\phi_1'(0)$, which is the maximum of the first harmonic's

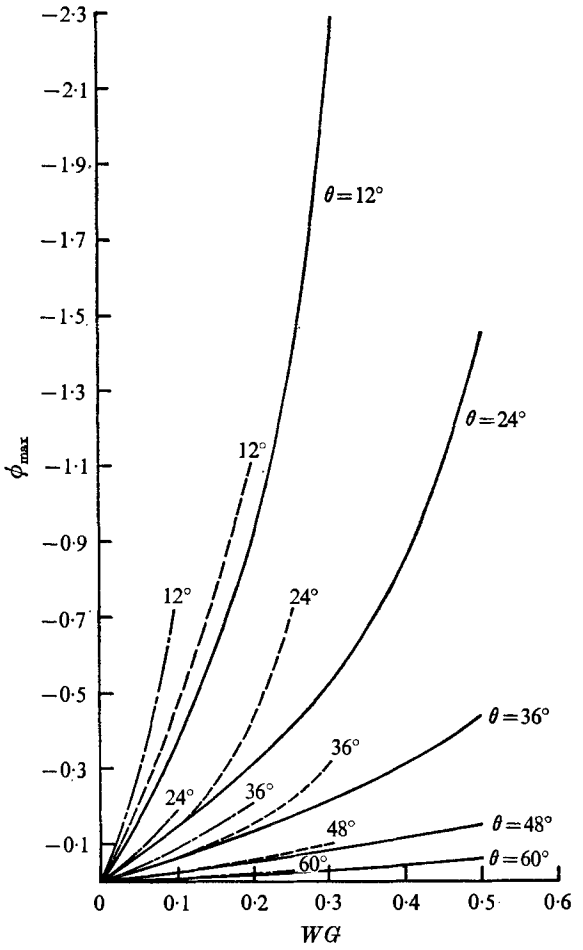

FIGURE 5. Maximum value of $\phi_1(z)$ as a function of θ, ϵ and WG. This is the peak vertical velocity (considering only the first harmonic) in the circulation cell, and is also a measure of the total volume flow rate of overturning in a single cell.

contribution to the spanwise surface current, as a function of WG, θ and ϵ. Figure 5 is a similar plot of the maximum value of $\phi_1(z)$; this is a measure of the total volume rate of overturning in a single Langmuir cell.

Figures 3–5 all show a rapid increase in the intensity of Langmuir cell motions as the angle θ is reduced (or as WG is increased). Although this is not indicated in the figures our calculations show that the disturbance reaches a maximum (for fixed WG and ϵ) at a small value of θ, and vanishes for $\theta = 0$.

Figures 6(*a*) and (*b*) give the same information as figures 3–5 but for $\epsilon = 0{\cdot}1$ and $0{\cdot}2$. Convergence difficulties for these larger values of ϵ are evident in this figure. The iterations converged here only for small values of WG.

Streamlines in the y,z plane are shown in figure 7 for $\epsilon = 0{\cdot}025$, $WG = 0{\cdot}4$ and $\theta = 24°$. The wave-slope parameter ϵ is too small for the asymmetries associated with higher harmonics to be evident.

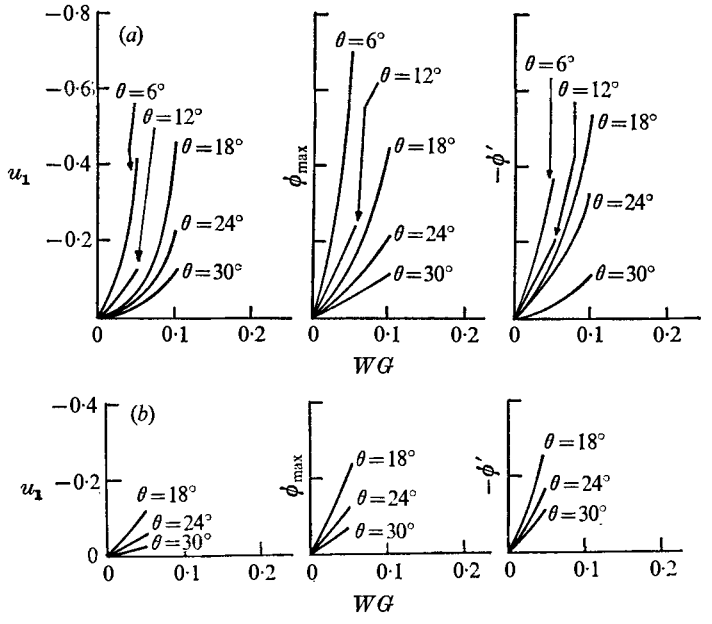

FIGURE 6. $u_1(0)$, maximum value of $\phi_1(z)$ and $\phi_1'(0)$ as functions of θ, ϵ and WG. (*a*) $\epsilon = 0{\cdot}1$. (*b*) $\epsilon = 0{\cdot}2$.

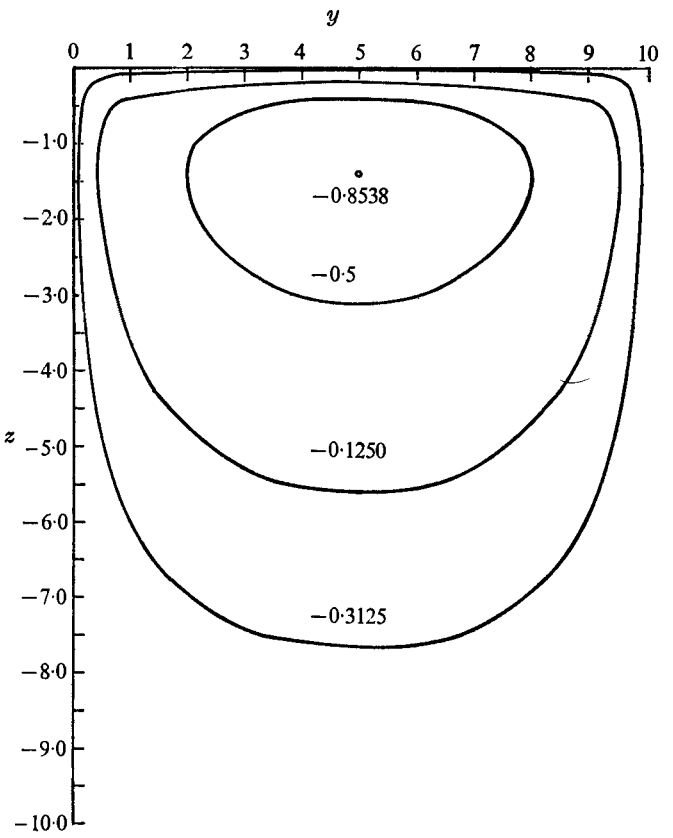

FIGURE 7. Streamlines for $\theta = 24°$, $WG = 0{\cdot}4$ and $\epsilon = 0{\cdot}025$.

8. Discussion

The present model, despite its limitations, contains the qualitative features LC (1)–(5) listed in §2. LC (1) and (2) are of course implicit in the form of the model. That is, the model is restricted to vortices aligned with the wind [LC (1)]. Spanwise periodicity of the vortices and the connexion with the wind as the energy source [LC (2)] arise from the assumption that short-crested wind-generated waves (with a discrete directional frequency spectrum) cover the surface.

LC (3) stems from a belief that the downwelling velocity beneath converging surface currents in Langmuir circulations exceeds the upwelling velocity below diverging surface currents (see Assaf *et al.* 1971, figure 23; Scott *et al.* 1969, figure 10). The evidence for this consists mainly of isotherm plots during the early stages of development of the circulation. This asymmetry in the cells is a feature of our numerical solutions, as may be seen in figure 1, which is typical. Near the surface the second harmonic has the same sign as the first harmonic. Thus, over downwelling zones near the surface the two harmonics reinforce each other, enhancing downwelling, while over upwelling zones they interfere and weaken upwelling. The second harmonic is unlikely to be particularly small for realistic wind speeds and wave slopes, and so considerable asymmetry might occur. Unfortunately, our solution procedure fails to converge for such cases. Accordingly, our results show the correct trend towards asymmetry, but do not provide definite confirmation of LC (3).

If $\mathscr{S}_d < 0$ [see (55)], then the downwelling zones in our model are situated below regions where the wind-directed surface current is greatest, while the upwelling zones are positioned below regions where the surface current is least. The tick marks on figure 3 indicate values of the wind speed parameter WG at which $\mathscr{S}_d = 0$; for WG exceeding this value, $\mathscr{S}_d < 0$ and property LC (4) is obtained. Clearly, the model also allows $\mathscr{S}_d > 0$, in which case property LC (4) is reversed. Whether this is the correct physical behaviour for low wind speeds is unknown, for well-organized LC's occur only for WG greater than about 0·3 (wind speeds exceeding 3 m/s).

Property LC (5) is indicated by the observations of Scott *et al.* (1969) that downwelling speeds are about $0{\cdot}0085W$ for $W > 3$ m/s, for this is comparable with an expected mean surface current of $0{\cdot}033W$. To discover whether our model satisfies LC (5) we must compare $0{\cdot}033W$ with $\epsilon^2 c\phi_{\max}$ (from figure 5), which represents the maximum downwelling speed due to the first harmonic. The case illustrated in figures 1 and 2 has $\epsilon^2\phi_{\max} = 1{\cdot}75 \times 10^{-3}$; since $c = O(W)$, this is rather too small. However, $\phi_{\max}$ increases with both ϵ and W in our calculations, and it is fairly evident that LC (5) will hold for realistic values of ϵ and W (for instance, $W \geqslant 3$ m/s and $0{\cdot}1 \leqslant \epsilon \leqslant 0{\cdot}4$). Unfortunately, our numerical procedure fails to converge when W and ϵ simultaneously have such typical values.

We attribute no physical significance to the divergence of our numerical method when this occurs. As indicated in § 5, convergence of the present numerical procedure is linked to the convergence of the series (46). We would expect to

be able to continue our results beyond the radius of convergence (in ΛR^2) of (46) by use of a finite-difference representation of (36).

Quantitative comparisons of our results with observational data are inevitably tentative, partly on account of the incomplete nature of the observations, partly because of the limitations of the computational method, and also because of the simplifications assumed in arriving at our final equations. On the observational side, for example, attempts at comparison are frustrated by the lack of reliable information concerning the gravity-wave spectrum when LC's are observed. The main simplifications in the theory are the assumptions of constant eddy viscosity, the invocation of an empirical $U_h'(z)$, and the statistical model of the directional spectrum of the waves (in which their random nature is assumed to be accounted for by a uniformly distributed random phase). Some of these simplifications may perhaps be removed and still yield a tractable model.

In fetch-limited situations, it is possible that prominent wave pairs may determine the LC cell spacing. However, we are convinced that the dominant cell spacings in the open sea or large lakes must normally be the outcome of a stochastic process. We hope that the statistical model of §6 is relevant to this situation despite its simplifications. For the particular 'spectrum' examined, the predicted average cell spacing is rather more than twice the wavelength of the dominant surface waves. The average cell spacing associated with less simple directional wave spectra may readily be calculated (although more labour is required), but it seems that our own crude estimate is not sensitive to slight changes in the directional properties of the spectrum.

This work was supported in part by NOAA Office of Sea Grant, U.S. Department of Commerce, under Grant GK-15-8102A. One of us (A.C.) also received a travel grant from the Science Research Council.

Appendix

The basic numerical scheme is described in §4. More information is supplied here.

Equations (42), truncated at $n = N$, were integrated using Simpson's rule, Newton's $\frac{3}{8}$ rule or a combination of these rules. The truncation error was of fifth order. Two-hundred grid points were used with a step size H in the z direction of 0·05. Convergence of the iterations was measured by the quantity

$$E = \sum_{n=1}^{N} \left| 1 - \frac{{}^{(j)}\phi_n'(0)}{{}^{(j+1)}\phi_n'(0)} \right|$$

(here iterates are indicated by a superprefix). The iterations were terminated when $E < 0{\cdot}01$ (in which case convergence was declared), or if E increased for successive pairs of iterates (in which case divergence was declared).

REFERENCES

ASSAF, G., GERARD, R. & GORDON, A. L. 1971 Some mechanisms of oceanic mixing revealed in aerial photographs. *J. Geophys. Res.* **76**, 6550–6572.

BOWDEN, K. F. 1950 The effect of eddy viscosity on ocean waves. *Phil. Mag.* **41** (7), 907–917.

BYE, J. A. T. 1965 Wind-driven circulation in unstratified lakes. *Limnol. Oceanogr.* **10**, 451–458.

BYE, J. A. T. 1967 The wave-drift current. *J. Mar. Res.* **25**, 95–102.

CRAIK, A. D. D. 1970 A wave-interaction model for the generation of windrows. *J. Fluid Mech.* **41**, 801–821.

CRAMÉR, H. 1937 *Random Variables and Probability Distributions.* Cambridge University Press.

ELLISON, T. H. 1956 Atmospheric turbulence. In *Surveys in Mechanics* (ed. G. K. Batchelor & R. M. Davies), p. 409. Cambridge University Press.

FALLER, A. J. 1971 Oceanic turbulence and the Langmuir circulations. *Ann. Rev. Ecology Systematics*, **2**, 201–236.

HIDY, G. M. & PLATE, E. J. 1966 Wind action on water standing in a laboratory channel. *J. Fluid Mech.* **26**, 651–688.

ICHIYE, T. 1967 Upper ocean boundary-layer flow determined by dye diffusion. *Phys. Fluids Suppl.* **10**, S270–S277.

KEULEGAN, G. H. 1951 Wind tides in small closed channels. *J. Res. Nat. Bur. Stand. Wash.* **26**, 358–381.

LANGMUIR, I. 1938 Surface motion of water induced by wind. *Science*, **87**, 119–123.

LEIBOVICH, S. & ULRICH, D. 1972 A note on the growth of small scale Langmuir circulations. *J. Geophys. Res.* **77**, 1683–1688.

LONGUET-HIGGINS, M. S. 1962 The statistical geometry of random surfaces. In *Hydrodynamic Stability. Proc. 13th Symp. Appl. Math.* pp. 105–144. Providence, R.I.: Am. Math. Soc.

LONGUET-HIGGINS, M. S. 1969 On wave breaking and the equilibrium spectrum of wind-generated waves. *Proc. Roy. Soc.* A **310**, 151–159.

MASCH, F. D. 1963 Mixing and dispersion of wastes by wind and wave action. *Int. J. Air Wat. Poll.* **7**, 697–720.

MYER, G. E. 1971 Structure and mechanism of Langmuir circulations on a small inland lake. Ph.D. dissertation, State University of New York at Albany.

PHILLIPS, O. M. 1963 A note on the turbulence generated by gravity waves. *J. Geophys. Res.* **66**, 2889–2893.

PHILLIPS, O. M. 1966 *Dynamics of the Upper Ocean.* Cambridge University Press.

RICE, S. O. 1944 The mathematical analysis of random noise. *Bell Syst. Tech. J.* **23**, 282–332, **24**, 46–156. (Reprinted in *Selected Papers on Noise and Stochastic Processes* (ed. N. Wax). Dover, 1954.)

SCOTT, J. T., MYER, G. E., STEWART, R. & WALTHER, E. G. 1969 On the mechanism of Langmuir circulations and their role in epilimnion mixing. *Limnol. Oceanog.* **14**, 493–503.

STEWART, R. W. 1967 Mechanics of the air–sea interface. *Phys. Fluids Suppl.* **10**, S 47–55.

STOMMEL, H. 1951 Streaks on natural water surfaces. *Weather*, **6**, 72–74.

SVERDRUP, H. U., JOHNSON, M. W. & FLEMING, R. H. 1942 *The Oceans*, pp. 481–482. Prentice-Hall.